

# PATH PLANNING FOR EDDY CURRENT INSPECTION AROUND PROBABLE DEFECTS

P. Olivieri (a), L. Birglen (a), X. Maldague (b), I. Mantegh (c)

(a) Polytechnique Montreal, Montreal QC, [pierre.olivieri@polymtl.ca](mailto:pierre.olivieri@polymtl.ca), (514) 340-5121 (ext. 2234)

(b) Laval University, Quebec QC

(c) NRC Aerospace Manufacturing Technologies Centre, Montreal QC

## Abstract

Part quality is an important aspect in the aerospace industry in order to avoid unpredictable and irreversible damages, and to ensure a long lifecycle. To ensure quality, non destructive testing (NDT) techniques are applied on parts and one of the most frequently used in the aerospace industry is eddy current testing (ECT). However, the latter is still mainly performed manually, entailing high costs in addition to be time-consuming. In this case, reliability and repeatability of inspection results are also limited due to their high dependence on the human operator. As part of an effort to robotize ECT with a 6 DOF manipulator arm and thus, free oneself from the many drawbacks of manual inspections, the authors previously proposed a coverage path planning methodology dedicated to complex aeronautical surfaces. However, orientation of the probe along these paths were not initially considered during this previous work while it is as much important as position information given that the probe must keep a normal orientation with respect to the surface to inspect it reliably. Following on from this previous work, the computation of these orientations along every point of the path is presented in this paper. Furthermore, another coverage path planning methodology is developed to inspect with ECT around a probable defect whose position is assumed to be known a priori. Once positions and orientations along inspection paths are computed, a simulation with a robotic simulation software (MotoSim) is made to generate the joint trajectories of a manipulator arm MotoMan SV3XL and teach it the automated inspection task. Afterwards, experiments using this manipulator with a mock-up representing a probe is realized. After these first experiments, it is observed that the motion of the robot is what one can expect during an efficient inspection around a known indication.

## Résumé

La qualité des pièces est un critère important dans l'industrie aérospatiale pour éviter des dommages imprévisibles et irréversibles et assurer un long cycle de vie. Pour cela, des techniques de contrôle non-destructif (NDT) sont utilisées, en particulier la technique d'inspection par courants de Foucault (ECT) qui est fréquemment employée sur les pièces aérospatiales. Cependant, cette technique est encore principalement réalisée manuellement et entraîne alors des coûts et un temps d'opération importants. De plus, les résultats d'inspection deviennent fortement dépendants de chaque opérateur humain ce qui limite ainsi leur fiabilité et leur répétabilité. Dans le cadre d'une solution de robotisation de ECT à l'aide d'un bras manipulateur à 6 DDL pour s'affranchir des inconvénients liés à l'inspection manuelle, les travaux présentés précédemment par les auteurs ont proposé une méthodologie de génération de chemins de couverture sur des surfaces aéronautiques complexes pour guider une sonde à courants de Foucault et réaliser l'inspection sur la surface d'intérêt. L'orientation de cette sonde le long des chemins n'était pas considérée dans ces travaux, mais constitue également un aspect particulièrement important car la sonde doit être maintenue normale à la surface le long de ces chemins. Dans la continuité de ces travaux, le calcul des référentiels d'orientation associés à chaque point du chemin est présenté dans cet article. Par ailleurs, une autre méthodologie de génération de chemins de couverture est présentée pour l'inspection autour d'un défaut probable dont la position sur la surface est connue à l'avance. Une fois les positions

et orientations calculées le long de ces chemins, les trajectoires d'un bras manipulateur MotoMan SV3XL qui permettront de suivre ces chemins sont ensuite déduites à l'aide d'un logiciel de simulation robotique (MotoSim). Enfin, un test expérimental sur le robot précédemment simulé est effectué en remplaçant la sonde par une maquette représentative de celle-ci. À la suite de ce test, les trajectoires du robot sont, à première vue, celles attendues pour réaliser une inspection efficace autour d'une indication.

## Introduction

Quality of parts is a critical objective in the aerospace industry, both during fabrication and maintenance processes, as it ensures them a long lifecycle. Especially, integrity of parts is controlled by resorting to non destructive testing (NDT) techniques. Eddy current testing (ECT) is one of these techniques mainly used in the aerospace industry. It is employed to detect surface and near surface cracks appearing in conductive parts at an early stage in order to avoid the rupture of the latter. Its principle consists in placing a coil supplied with an alternative current towards the surface of a conductive part in order to induce circular currents (known as "eddy currents") at its surface and in its near surface. Thus, when a defect is present in front of the coil, eddy currents will be disrupted and the impedance of the coil will be perturbed as well. In practice, the device containing the coil is called eddy current (EC) probe and the measured signal corresponds to the impedance of the coil. As a result when a crack disrupts eddy currents, a variation of impedance is observed.

However, this technique is still mainly applied manually and it leads to decrease the reliability and repeatability of cracks detection as wobbles of the probe may involve noised signal. Also, in addition to be a hard, time-consuming and costly task when performed manually, human operators may be exposed to hazardous environments. In (Olivieri, Birglen, Maldague, & Mantegh, 2013), a solution using a 6 DOF manipulator arm with an EC probe mounted on its tool flange is proposed to robotize ECT and a path planning method is described to properly guide the probe in front of aeronautical surfaces such as shown in Figure 1 with a zigzag covering pattern. However, the computed paths, represented by an ordered list of points, are only expressed with position coordinates while orientation coordinates are not discussed. Orientation is as much important as position coordinates because the probe must be swept with a normal orientation along the surface to detect defects efficiently.

Following on from the work in (Olivieri, Birglen, Maldague, & Mantegh, 2013), orientation coordinates are computed to each point of the path in order to meet ECT's orientation constraints of the probe. Additionally, another strategy of inspection is investigated: a local inspection around a probable defect whose position on the surface is assumed to be known *a priori*. A path planning methodology is then presented to perform this local inspection. Finally, a simulation with robotic simulation software MotoSim is made and an experiment in a robotic cell using a manipulator arm MotoMan SV3XL is realized.

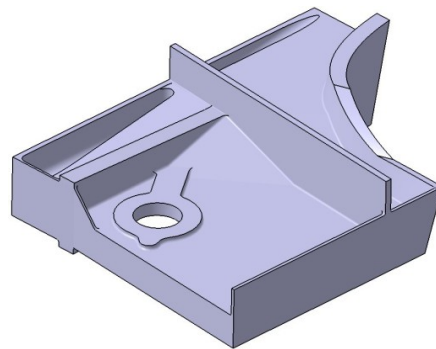


Figure 1: Part from the central barrel of an aircraft (Olivieri, Birglen, Maldague, & Mantegh, 2013).

## 1. Methodology of path planning for eddy current inspection tasks

### A. Inspection of a target surface

In a previous work (Olivieri, Birglen, Maldague, & Mantegh, 2013), a coverage path planning methodology is described to perform a robotized eddy current inspection dedicated to detect cracks on complex aeronautical surfaces. The Figure 1 displays the type of surfaces considered in this previous work and its 3D model is assumed to be known *a priori*. The main steps of this methodology are:

1. Tessellate the target surface of the model with triangular facets and export it in a stereolithography (STL) format.
2. Partition the surface into multiple patches (i.e. subsurfaces) with a geometry and topology simple enough to build zigzag paths on each of them by using the *section plane* approach (cf. Figure 2) without having irregular (or even inconsistent) paths. Based on (Atkar, Comer, Greenfield, Choset, & Rizzi, 2009), three successive segmentations are performed to partition this surface:
  - a. A segmentation based on the curvature of the surface and called “watershed segmentation” (Mangan & Whitaker, 1999).
  - b. A segmentation on previously obtained patches to limit their maximum deviation angle (i.e. the maximum angle formed between the normals of every pairs of their facets) with a threshold value, thus ensuring their flatness.
  - c. A segmentation based on topology using an algorithm known as “Morse decomposition”, (Acar, Choset, Rizzi, Atkar, & Hull, 2002).
3. Generate zigzag (or rastering) paths on each resultant patches by cutting them with regularly offset section planes (cf. Figure 2).

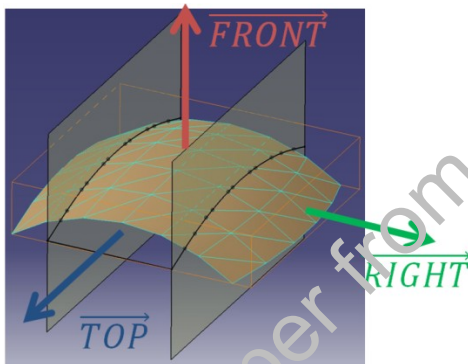


Figure 2: Zigzag path construction technique using section planes offset along the **RIGHT** direction.

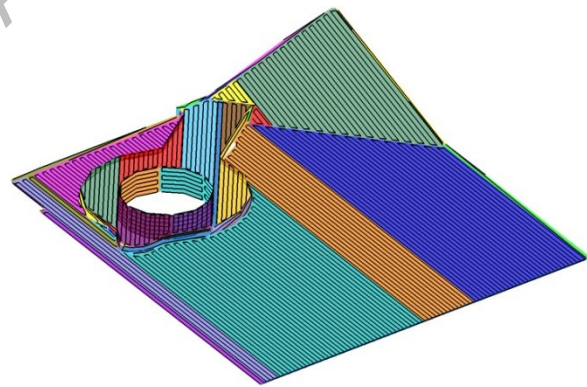


Figure 3: Zigzag paths on the different patches of the surface to inspect.

The result of this methodology on a surface of interest extracted from the aeronautical part illustrated in Figure 1 is displayed in Figure 3. Zigzag paths are built on each patch of the surface in order to perform a global inspection of this target surface using ECT. In the next subsection, another strategy of inspection frequently used with ECT is discussed and a path planning methodology of this strategy is presented.

### B. Inspection around an indication of a surface

Eddy current testing is a technique that has the advantage of being very sensitive to detect surface and near surface cracks compared with other existing NDT techniques. However, inspection using ECT can take a long time due to the small area covered by the EC probe. Thus, this technique is well adapted to diagnose a small area where a defect is suspected (NDT Education Resource Center). Penetrant testing (PT) on the other hand is another NDT technique that is useful to inspect large areas relatively fast with a high sensitivity to detect open cracks at the surface. However, this technique requires also an important attention during each of its steps (properly cleaning the surface, correct removal of the excess penetrant, etc.). Therefore, it is common to inspect suspicious areas that are in reality not a real defect (e.g. a spot of grease holding some penetrant similarly to a crack). This is why a finer inspection is often needed to confirm if the suspected areas (usually referred to as “indications”) correspond or not to a defect. Thus, this technique can be combined beneficially with ECT as the latter can sort out representative indications from the false ones.

In this subsection, a path planning methodology adapted to ECT to inspect around an indication is presented. Moreover, given that cracks are supposed to correspond in most cases to linear indications (cf. Figure 4(a)), a broken line model will be used and its position is assumed to be known (cf. Figure 4(b)).

Then, a path adapted to this indication is to sweep the probe with a zigzag pattern perpendicular to the segments of the line. Indeed, in the event that the indication is a real crack, its detection will be easier as eddy currents will be quickly disrupted along each pass and a large net variation of impedance of the probe will be observed (cf. Figures 5(a) and 5(b)).

To build a perpendicular zigzag path along an indication line, specific geometric parameters (cf. Figure 6) are defined by an operator to adapt the path to each situation. The following pseudo-code is then used:



Figure 4: (a) Indication (dotted circle) observed forming a bright green line under a black light (ultraviolet). (b) Zoomed view of the indication and its approximation as broken line segments.

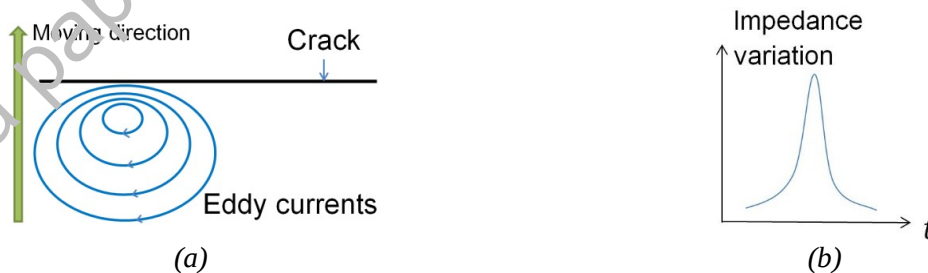


Figure 5: (a) Eddy currents are significantly disrupted as the probe is moved perpendicularly to the crack's line. (b) Amplitude of impedance variation of the probe along a motion perpendicular to a crack.

**Pseudo-code of path generation perpendicular to an indication:**

**Data:** Triangles and Vertices of the surface mesh, List of points  $(Pt_k)_{k=1...N}$  of an indication line segments, path parameters  $(d\_Ind, offset\_Ind, W\_Ind)$

**Result:** Inspection path perpendicular to the indication

Extrapolate extreme points  $Pt_0$  and  $Pt_{N+1}$  tangent to the indication so that extreme passes are distant of  $offset\_Ind$  from the first and last points  $Pt_1$  and  $Pt_N$ ;

Compute equidistant points  $(M_i)_{i=1...P}$  along the extrapolated line  $(Pt_k)_{k=0...N+1}$  with a fixed distance  $d\_Ind$  by considering  $M_1 = Pt_0$ . Add to the previous list  $M_{P+1} = Pt_{N+1}$ ;

Initialization:  $Path = []$ ;

for  $i=1$  to  $(P + 1)$

    Compute all intersection points  $IP$  between the triangle edges and  $P_i$ , the section plane perpendicular to the indication's line and passing through  $M_i$ ;

    Sort  $IP$  along one direction to form a new pass of the zigzag path;

    Select only points from  $IP$  such that the end points of the final pass are within a length of  $W\_Ind$  on both sides of the indication. Note  $IP_w$  this final pass;

    Add this pass in the zigzag path:  $Path = [Path; IP_w]$ ;

endfor

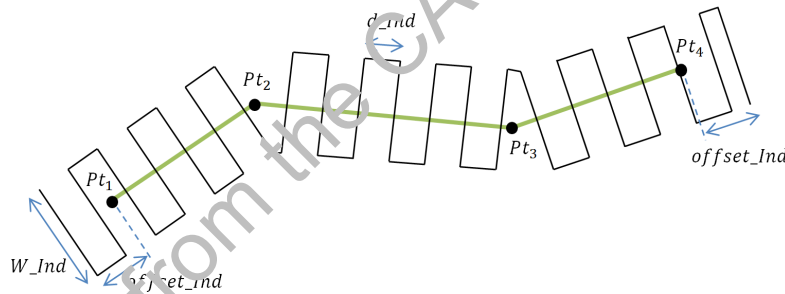


Figure 6: Path parameters of a perpendicular path of inspection around an indication.

The application of this methodology around a known indication located in a fillet of 2 mm of radius is illustrated in Figure 7.

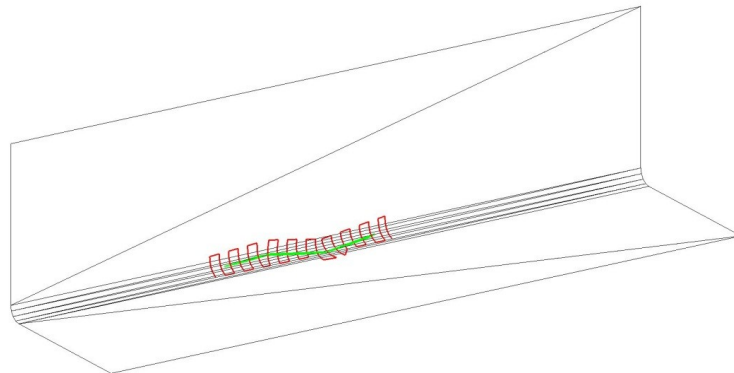


Figure 7: Zigzag path around a known indication to refine a diagnostic with ECT.

For both strategies of inspection presented so far, namely the inspections of a target surface and around a known indication, paths are described only with a list of coordinates of position, but the orientation of the probe along these paths was not discussed. It is yet critically important to guarantee the reliability of the probe signal. The next subsection deals with this issue.

### C. Orientation of the EC differential probe

In the present work, a *differential* EC probe is used since it is very sensitive to detect defects (NDT Education Resource Center). Compared to *absolute* EC probe that are composed of only one coil, the differential arrangement has two coils wound in opposition (cf. Figure 8(a)) and the signal measured from this probe is the difference of impedance between its two coils. As a result, the signal measured in front of a discontinuity such as a crack is amplified which makes detection easier. Moreover, common noise stemming from lift-off or wobbles is reduced with differential probes.

However, to optimize the signal integrity coming from these probes, two conditions on the orientation of the probe have to be satisfied along the inspection path:

1. The probe must be kept normal to the surface (cf. Figure 8(a)). Indeed, a tilt (even small) can add significant noise to the measured impedance;
2. The alignment of the two coils must be kept tangent to the path along each pass of the zigzag. Indeed, as illustrated in Figure 8(b), if one assumes two cracks: one parallel to the alignment of the coils (crack (1)), and another perpendicular to the latter (crack (2)), the differential signal will not change if the probe is swept perpendicularly to crack (1) as its two coils will see the same variation. On the other hand, this signal will change a lot if the probe is swept perpendicularly to the crack (2) (i.e. parallel to the alignment of its coils).



Figure 8: (a) The probe must be kept normal to the surface (NDT Education Resource Center) (b) Top view of a differential probe. The differential signal will not change if the probe is swept perpendicularly to crack (1) whereas this signal will change if swept perpendicularly to crack (2).

Let us note  $(\mathbf{n}^M, \mathbf{o}^M, \mathbf{a}^M)$  the orientation frame associated to the probe at a point  $M$  of the path. The vector  $\mathbf{a}^M$  is the approach direction of the probe aligned with its main axis,  $\mathbf{o}^M$  is the orientation direction of the probe. It is orthogonal to  $\mathbf{a}^M$  and collinear with the alignment of the two coils. Finally, the normal direction  $\mathbf{n}^M$  is obtained using the cross-product of the latter vectors such that  $(\mathbf{n}^M, \mathbf{o}^M, \mathbf{a}^M)$  is a right-handed orthogonal frame. Based on these definitions, the following pseudo-code is used to compute the orientation frame at each point  $M$  (cf. Figure 9):

**Pseudo-code to compute the orientation frame at each point of the path:**

**Data:** List of Patches, Triangles and Vertices of the surface mesh, point  $M$ , sweep direction **RIGHT** of the zigzag path

**Result:** right-handed orthogonal frame  $(\mathbf{n}^M, \mathbf{o}^M, \mathbf{a}^M)$

Estimate the normal to the surface  $\mathbf{n}_M$  at point  $M$ ;

Choose the approach direction  $\mathbf{a}^M$  as the opposite of  $\mathbf{n}_M$  in order to keep the probe normal to the surface:  $\mathbf{a}^M = -\mathbf{n}_M$ ;

Compute the orientation direction  $\mathbf{o}^M$  such that it is orthogonal to  $\mathbf{a}^M$  and oriented along the direction of passes (i.e. orthogonal to the sweep direction **RIGHT**):  $\mathbf{o}^M = \frac{\mathbf{a}^M \times \mathbf{RIGHT}}{\|\mathbf{a}^M \times \mathbf{RIGHT}\|}$ ;

Deduce the normal direction  $\mathbf{n}^M$  such that  $(\mathbf{n}^M, \mathbf{o}^M, \mathbf{a}^M)$  forms a right-handed orthonormal frame:  $\mathbf{n}^M = \mathbf{o}^M \times \mathbf{a}^M$ ;

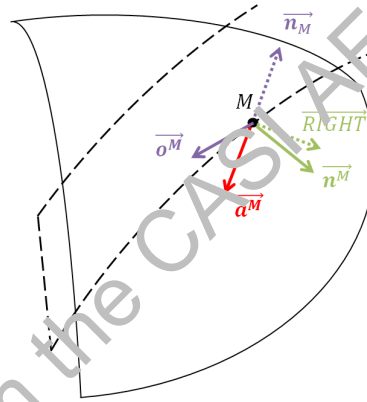


Figure 9: Orientation frame  $(\mathbf{n}^M, \mathbf{o}^M, \mathbf{a}^M)$  at point  $M$  of the path.

The first operation of this pseudo-code is to estimate the normal to the surface  $\mathbf{n}_M$  at point  $M$ . This operation is performed in two steps:

1. At each vertex  $Pt_j$  of the surface mesh, approximate the normal  $\mathbf{n}_{Pt_j}$  to the surface by averaging the normal  $\mathbf{n}_{T_i}$  of the neighboring triangles  $T_i$  weighted with the incident angle  $\theta_i$

to  $Pt_j$  (cf. Figure 10(a)):  $\mathbf{n}_{Pt_j} \cong \frac{\sum_i \theta_i \mathbf{n}_{T_i}}{\|\sum_i \theta_i \mathbf{n}_{T_i}\|}$ . This method is adapted from (Thürner &

Wüthrich, 1998);

2. Deduce the normal  $\mathbf{n}_M$  at point  $M$  by interpolating linearly between the normals at the vertices  $Pt_1$  and  $Pt_2$  corresponding to the triangle's edge containing  $M$  (cf. Figure 10(b)): as

$M = Pt_1 + t(Pt_2 - Pt_1)$  with  $t \in [0; 1]$ , the normal at this point is approximated by  $\mathbf{n}_M \cong \mathbf{n}_{Pt_1} + t(\mathbf{n}_{Pt_2} - \mathbf{n}_{Pt_1})$ .

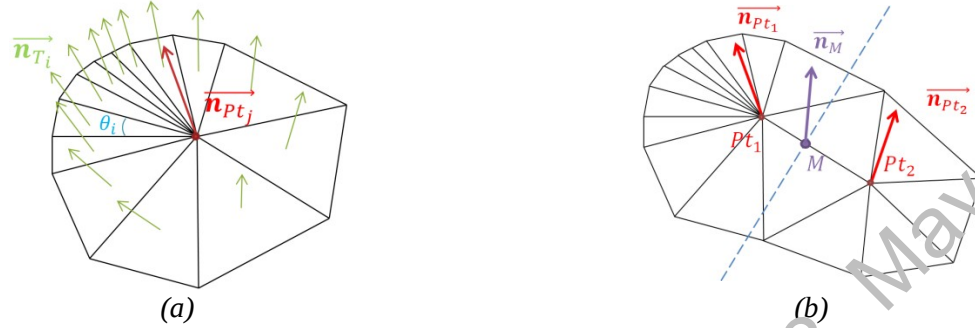


Figure 10: (a) Approximation of the normal vector at each vertex of the surface mesh (Thürrner & Wüthrich, 1998). (b) Approximation of the normal vector at a point  $M$  of the path by linear interpolation between the normals at the end points of the edge containing  $M$ .

The estimation of the orientation frame attached to each points of the path in Figure 7 is illustrated in Figure 11.

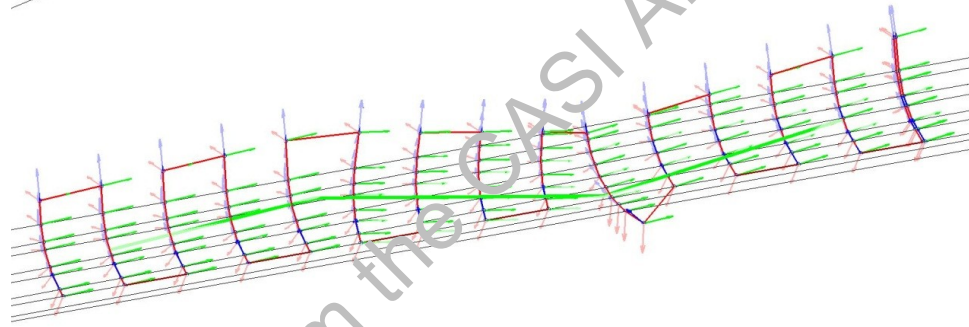


Figure 11: Orientation frames  $(\mathbf{n}^M, \mathbf{o}^M, \mathbf{a}^M)$  computed along each point of the path.

## 2. Simulations on a robotic simulation software

After computing an inspection path in terms of position and orientation that must be followed by the end of the EC probe, a simulation of this path is performed using MotoSim (version 6.4), a robotic simulation software. More precisely, a 6 DOF manipulator (MotoMan SV3XL) is simulated with an EC probe of 150 mm (represented in blue in Figure 12(a)) mounted on its tool flange so that the end of the probe follows the computed path (Figure 12(b)) to inspect around a known indication in a fillet of 2 mm of radius. The interest of simulating the path is, at first, to compute the trajectory of the robot by defining the type of motion and the speed along the path and export this trajectory in a file readable by the controller of the real robot. Moreover, this tool software is useful to detect collisions, if any, and check if the computed path can be actually reached by the robot (taking into account the joint limits, singularities, etc.). Results of this simulation (Figure 12) are obtained for example with a linear motion between each point of the path and a linear speed of  $2 \text{ mm.s}^{-1}$  at the end of the probe.

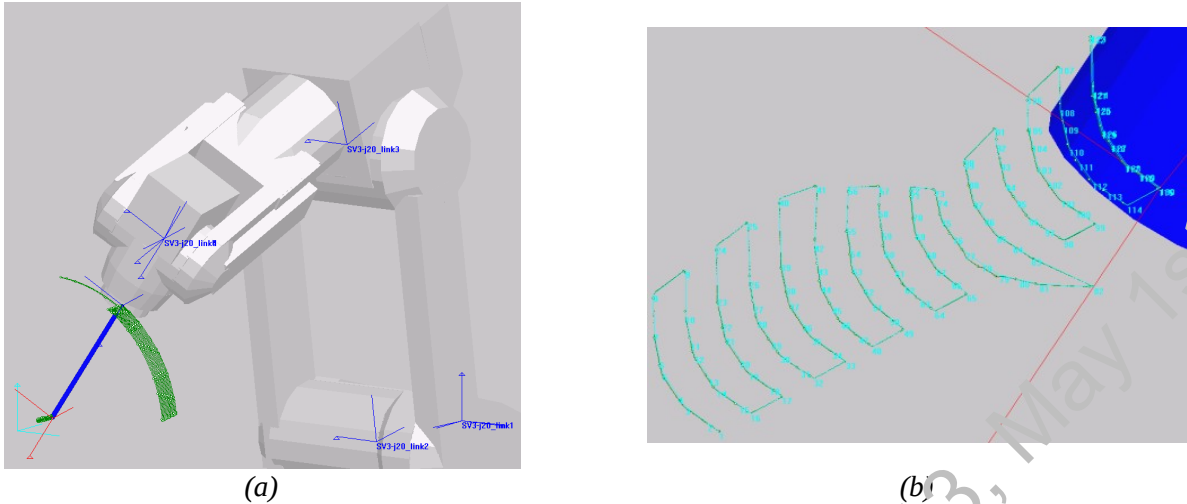


Figure 12: (a) Simulation of an EC inspection around an indication in a fillet of 2 mm of radius (surface not represented here) using a 6 DOF manipulator MotoMan SV3XL. (b) Zoomed view at the end of the EC probe (blue).

### 3. Experiment

Once the trajectory generated by the simulation with MotoSim and exported in a proper file format, the latter is then loaded in the robot controller (XRC 2001) and the manipulator arm MotoMan SV3XL with 6 DOF can execute the taught operation. In Figure 13(a), the arm MotoMan SV3XL is shown handling a mock-up used to simulate an EC probe (cf. Figure 13(b)), and is executing the inspection trajectory around a known indication in a virtual fillet of 2 mm of radius. Though this fillet is not really used in the experiment and that a mock-up is mounted on the robot flange instead of a real EC probe, visual results of the robot motion are what one expected to perform a proper inspection with ECT on this fillet.



Figure 13: (a) Manipulator arm MotoMan SV3XL handling a mock-up used to simulate an EC probe and inspecting around an indication of a virtual fillet of 2 mm of radius. (b) Zoomed view at the end of the mock-up.

### Conclusion

With this article, a methodology for path planning generation adapted for eddy current inspections was presented. Two strategies of inspection are considered for path planning: the global inspection of a target surface and the local inspection around a probable defect (referred to as an “indication”) whose position is known *a priori*. The methodology previously used to generate paths for a global inspection is taken from (Olivieri, Birglen, Maldague, & Mantegh, 2013). The target surface is first approximated by a

triangular mesh. Then, the latter is partitioned into several patches so that regular and consistent paths can be built on each of them by using a “section planes” technique. Finally, this technique is applied to generate a covering zigzag path on each patch and consequently, inspect the whole target surface. A second methodology is also developed to inspect locally around a known indication, and consists in building a zigzag path with every pass set perpendicular to the polygonal line modeling this indication. Similarly to the previous methodology, paths are built by intersecting each patch with section planes perpendicular to the broken line of the indication, and regularly spaced along this line. Parameters are also defined to let the user adjust dimensions of the path for each situation. Once the path is computed, the orientation frame associated to each point of the path is deduced and a simulation with robotic simulation software (MotoSim) is performed to get trajectory (path expressed with the time) followed by a manipulator arm (MotoMan SV3XL). Afterwards, an experiment is realized with the robot considered in the simulation by loading the trajectory in the robot’s controller.

In this article, an experiment simulating an inspection around an indication in a fillet of 2 mm of radius is illustrated. Though the robot is actually manipulating a mock-up similar to a probe, and a virtual fillet is considered during the experiment, the motion of the robot is what can be expected at first sight to perform an effective eddy current inspection around an indication. However, further experiments using a real probe and considering a real surface will validate the developed methodologies.

### Acknowledgments

This work was supported by the Natural Sciences and Engineering Research Council of Canada (NSERC) and the Consortium de recherche et d’innovation en aérospatiale au Québec (CRIAQ). The authors also gratefully thank their industrial partners L-3 Communications, Pratt & Whitney Canada, and NRC for their financial support and their useful suggestions throughout this work.

### References

- Acar, E. U., Choset, H., Rizzi, A. A., Atkar, P. N., & Hull, D. (2002). Morse Decomposition for Coverage Tasks. *The International Journal of Robotics Research* , Vol. 21, No. 4, pp. 331-334.
- Atkar, P. N., Conner, D. C., Greenfield, A., Choset, H., & Rizzi, A. A. (2009). Hierarchical Segmentation of Piecewise Pseudoextruded Surfaces for Uniform Coverage. *IEEE Transactions on Automation Science and Engineering* , Vol. 6, No. 1.
- Mangan, A. P., & Whitaker, R. T. (1999). Partitioning 3D Surface Meshes Using Watershed Segmentation. *IEEE Transactions on Visualization and Computer Graphics* , Vol. 5, No. 4.
- NDT Education Resource Center. (n.d.). *Probes - Mode of Operation*. Retrieved 01 23, 2013, from NDT Resource Center: <http://www.ndt-ed.org/EducationResources/CommunityCollege/EddyCurrents/ProbesCoilDesign/ProbesModeOp.htm>
- NDT Education Resource Center. (n.d.). *Surface Breaking Cracks*. Retrieved 04 24, 2013, from NDT Resource Center: <http://www.ndt-ed.org/EducationResources/CommunityCollege/EddyCurrents/Applications/breakingcracks.htm>
- Olivieri, P., Birglen, L., Maldague, X., & Mantegh, I. (2013). Coverage path planning for eddy current inspection on complex aeronautical parts. *Robotics and Computer Integrated Manufacturing, submitted on January 18th 2013* .

Thürner, G., & Wüthrich, C. A. (1998). Computing Vertex Normals from Polygonal Facets. *Journal of Graphics Tools* , 3 (1), 43-46.

Preprint of a paper from the CASI AERO'13, May 1st 2013